HHS Public Access

Author manuscript

Acta Biomater. Author manuscript; available in PMC 2021 September 15.

Published in final edited form as:

Acta Biomater. 2020 September 15; 114: 407–420. doi:10.1016/j.actbio.2020.07.006.

Controlled Release of Soy Isoflavones from 3D Printed Bone Scaffolds for Bone Tissue Engineering

Naboneeta Sarkar, **Susmita Bose***

W. M. Keck Biomedical Materials Research Laboratory, School of Mechanical and Materials Engineering, Washington State University, Pullman, Washington 99164, United States

Abstract

Recent challenges in post-surgical bone tumor management have elucidated the need for a multifunctional scaffold, which can be used for residual tumor-cell suppression, defect repair, and simultaneous bone regeneration. In this perspective, 3D printing allows to create a wide variety of patient-specific implant with complex porous architecture and compatible mechanical strength to that of cancellous bone. Here, a multifunctional bone graft substitute is designed by incorporating the three primary soy isoflavones: genistein, daidzein, and glycitein onto a 3D printed (3DP) tricalcium phosphate (TCP) scaffolds with designed pores, endowing them with *in vitro* chemopreventive, bone-cell proliferating and immune-modulatory potential. The interconnected porosity and biodegradability of 3DP TCP ceramics have allowed a controlled release kinetics of genistein, daidzein and glycitein in acidic and physiological buffer medium for 16 days, which is fitted with Korsmeyer-Peppas model. Presence of genistein, a well-known natural biomolecule shows a 90% reduction *in vitro* osteosarcoma (MG-63) cell viability and proliferation after 11 days. Meanwhile, daidzein, the other primary isoflavone, promotes *in vitro* cellular attachment and enhances viability and proliferation of human fetal osteoblast cell (hFOB). Furthermore, controlled release of genistein, daidzein, and glycitein from 3DP TCP scaffold demonstrates improved hFOB cell proliferation, viability, and differentiation in a dynamic flow-perfusion bioreactor, which is utilized to better simulate the clinical microenvironment. Finally, *in vivo* H&E staining confirms controlled co-delivery of genistein-daidzein-glycitein from 3DP scaffold carefully modulated neutrophil recruitment to the surgery site after 24 hours of implantation in a rat distal femur model. These results advance our understanding towards multipronged therapeutic approaches utilizing synthetic bone graft substitutes as a drug delivery vehicle, and more importantly, demonstrate the feasibility of localized tumor cell suppression and bone cell proliferation for post-surgical defect repair application.

Graphical abstract

* sbose@wsu.edu, Phone: (509) 335-7461.

Declaration of interests

The authors declare that they have no known competing financial interests or personal relationships that could have appeared to influence the work reported in this paper.

Data availability

Data will be made available upon request.

Graphical Abstract

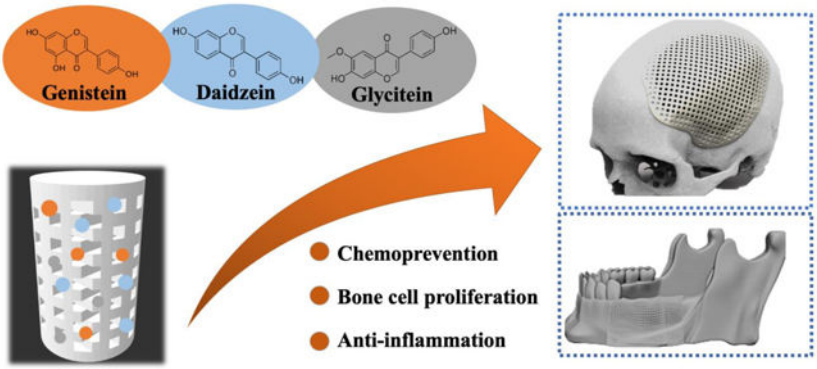

Keywords

3D printed TCP; Drug delivery; Soy isoflavones; Flow perfusion bioreactor; In vivo

1. Introduction

Despite current medical advances in cancer management, the treatment of osteosarcoma and metastatic bone cancer still remains a challenge. Osteosarcoma is the most common primary bone malignancy and the mainstay of its therapeutic treatment are pre- and postoperative chemotherapy with limb-salvaging surgery. [1] The surgical resection often fails to eradicate residual malignant cells, which leads to tumor recurrence. Besides, it creates large bone defects, which bone cannot repair by itself. The reconstruction of lost bone also involves acute inflammation, which minimizes the regenerative efficacy and subsequently leads to delayed fracture repair. Furthermore, pre- and post-operative chemotherapy cause significant side effects and drug-resistance. Therefore, successful treatment of post-surgical defect-repair relies on a multifunctional approach involving tissue regeneration, chemoprevention, and anti-inflammation.

Bone tissue engineering (BTE) is an alternative treatment for bone-defect repair, which holds great promise for promoting bone regeneration and overcoming some of the drawbacks of conventional techniques. [3–5] Due to the variable location of tumors and their proximity with surrounding bone tissues, osteosarcoma resection faces considerable challenges. To overcome this challenge in precise osteosarcoma resection, computer-aided design (CAD) was used to design patient-specific prosthesis on the basis of the computer tomography (CT) scan and magnetic resonance imaging (MRI) of the osteosarcoma of human patients. Then 3D printing technique are being used to fabricate the 3D printed prosthesis which perfectly fit to the bone defect. Recently, 3D printing technology has revolutionized the conventional concepts of oncological surgery and made it possible to accurately remove tumors and perform patient-specific reconstruction. In addition to anatomical models and surgical guides, 3D-printed prostheses have been approved for clinical trials and achieved certain success. There is an emerging interest in using 3D printed (3DP) porous tricalcium phosphate (TCP) scaffold due to its appropriate *in vivo* degradation rate which matches the speed of bone tissue ingrowth. [6] Moreover, it has excellent

biocompatibility, osteoconductivity and compositional similarity to the bone, which imparts significant advantages onto TCP compared to other biomedical materials. [7] 3DP scaffold with high porosity and homogeneous interconnected pore have been extensively used in BTE due to their effectiveness in oxygen-nutrient transport, waste removal, and vascularization. [8] Local drug delivery from tissue-engineered scaffold could facilitate the release of high concentrations of chemopreventive agents at tumor sites and minimize the cytotoxicity to normal cells. [9]

Soy, often referred to as “miracle crop” for its versatile uses, have been a staple diet in Southeast Asia for centuries. [10] Soybeans and its products are the greatest dietary source of isoflavones, one of the most common forms of phytoestrogens, or plant-derived estrogens. [11] The three primary isoflavones found in soybean are genistein, daidzein, and glycitein, which account for 50, 40 and 10% of the total isoflavone content, respectively. [12–13] Decades of research and epidemiological investigations have linked soy consumption to a variety of potential health benefits, including reduced risk for cardiovascular diseases, obesity-related metabolic syndrome, several types of carcinogenesis such as breast and prostate cancers as well as alleviated menopausal symptoms and improved bone health. [14–17]

Genistein (4,5,7- trihydroxyisoflavone), one of the major soy isoflavones, demonstrated a wide range of biological activities but it is best recognized for its ability to impede cancer growth without being toxic to normal cells. [18] It has been shown to inhibit the growth of various cancer cell lines including; breast, lung, prostate, leukemia, lymphoma, and head and neck cancer cells, both *in vitro* and *in vivo.* [19–23] Daidzein (4,7- dihydroxyisoflavone), the other chief isoflavones, has also received increasing attention due to its possible role in osteoporosis prevention. The estrogenic effects of daidzein have been proposed to reduce bone resorption and improve bone mineral density. [24] Recent reports revealed increased osteoblast viability, alkaline phosphatase (ALP) activity and osteocalcin synthesis in presence of daidzein. [25] Furthermore, soy isoflavones, mainly genistein and daidzein, have consistently proven to exhibit immunomodulatory potentials in numerous *in vitro*, *in vivo* and pre-clinical studies. [26–29] The underlying mechanism explaining the immunomodulatory activities include inhibition of NF-κβ pathway and subsequent downregulation of pro-inflammatory cytokine production.[30]

Although the vast majority of *in vitro* cell culture is designed in a conventional static system, they do not offer vascular blood supply or nutrient delivery to the cells, limiting the cellular activity at the center of 3DP BTE scaffolds. [31] To simulate the aspects of the *in vivo* environment, flow perfusion bioreactors play a crucial role by enhancing the nutrient exchange and generating the mechanical stimuli in the form of flow-mediated shear stress. [32–33] They allow perfusion of culture medium through the interconnected pores of 3DP TCP scaffolds, thereby enhancing cell viability, proliferation, and extracellular matrix production.

In the context of these reports, a combination of isoflavones, containing genistein, daidzein, and glycitein in 5:4:1 ratio was utilized in this study, in order to mimic their original proportion in soy isoflavones. We integrated soy isoflavones with 3DP TCP scaffolds with

designed porosity to form a multifunctional BTE scaffold for post-surgical tumor resection. *In vitro* release of soy isoflavones, genistein and daidzein were obtained from TCP scaffolds. Human fetal osteoblast cells (hFOB) and human osteosarcoma (MG-63) cells were cultured on soy isoflavone loaded TCP scaffold in a static and dynamic system. The aims of this work are (i) to understand the release kinetics of soy isoflavones from the porous 3DP scaffold, (ii) to evaluate *in vitro* osteoblast proliferating and osteosarcoma preventing efficacy of soy isoflavones, (iii) to compare dynamic flow-perfusion bioreactor system with the static cell culture, and (iv) to investigate the efficacy of soy isoflavones at post-surgical inflammatory sites in rat distal femur model. We hypothesized the presence of soy isoflavone genistein will prevent *in vitro* osteosarcoma proliferation, whereas daidzein will enhance the *in vitro* osteoblast proliferation and together they may control inflammatory cell recruitment at the implantation site. Moreover, the controlled release of soy isoflavones will induce *in vitro* chemoprevention, osteoblast cell proliferation and modulate post-surgical neutrophil recruitment in rat distal femur model.

2. Experimental

2.1 3D printed scaffold preparation

The porous TCP scaffolds were fabricated by binder jetting technique. At first, pure ß-TCP powder was synthesized by solid-state synthesis method. Briefly, a homogeneous mixture of calcium carbonate ($CaCO_3$, 1 M) and calcium phosphate dibasic ($CaHPO_4$,2 M) was obtained after ball milling the powders for 2 hours. Calcination was carried out at 1050°C for 24 hours. The calcined powder was sieved and ball-milled for 6 hours using 2:3 W/V ethanol and 5:1 W/W zirconia ball to powder ratio. Ethanol was evaporated by heating the slurry overnight at 60°C. Resultant powder was sieved and used for fabricating 3D printed scaffolds. We have used a binder jet printer (ProMetal®, ExOne LLC, Irwin, PA, USA) to synthesize cylindrical scaffolds (d= 3.2 mm l=5 mm) with interconnected pores of 400 μm size. The CAD design had square-shaped pores penetrating orthogonally through the cylinder in X, Y and Z directions. A proprietary aqueous binder provided by the company was used for the built process. The fabricated green part was subjected to binder removal at 175°C for 90 min followed by depowderization by air blowing. Depowderization is a crucial and sensitive process which removes the loosely adhered powder that blocks the pores. Finally, the scaffolds are sintered at 1250°C in a conventional muffle furnace for 2 hours.

2.2 Drug loading and in vitro release of soy isoflavone

For *in vitro* release study, genistein, daidzein, and glycitein (Sigma Aldrich, MO) in 5:4:1 weight ratio was dissolved in ethanol at a concentration of 0.1 mg/ml. 100 μl of total drug solution was loaded on 3DP TCP scaffold. *In vitro* release study was performed at pH 7.4 and pH 5.0 that imitate the physiological pH and the acidic environment right after surgery, respectively (n=3). While acetate buffer solution served for pH 5.0 release media, pH 7.4 was represented by dulbecco's modified eagle medium (DMEM) supplemented with fetal bovine serum (FBS) to closely mimic the *in vitro* cell culture media. The DMEM contained high concentrations of amino acids and vitamins as well as some inorganic salts in a glucose-based media, which was supplemented with 10% FBS comprising various growth factors, proteins and hormones. A pH probe was used to ensure the measured pH was within

±0.05 range. Subsequently, implants immersed in 4 ml of buffer solution were placed in an orbital shaker at 150 rpm at 37°C. At each time point, buffer media was collected and then refilled with the respective pH buffer. Buffer media was collected after selected time points; 1.5, 3, 6, 12, 24 hours and then 2, 3, 5, 7, 10, 14, 18, and 21 days. The concentration of genistein, daidzein and glycitein released at selected time points were measured using a Biotek Synergy 2 SLFPTAD microplate reader (Bioteck, Winooski, VT, USA). Briefly, 200 μl of collected media was pipetted in a 96-well plate and the absorbances of each well were measured at 254 nm wavelength. Finally, drug concentration was measured using a standard curve and plotted against time.

2.3 In vitro static osteoblast and osteosarcoma cell culture study

All scaffolds were sterilized in an autoclave (Tuttnauer, USA) at 121°C for 60 min, prior to the *in vitro* cell culture studies. The osteosarcoma cell (MG-63, human osteosarcoma cell line) and the cell media (EMEM, Eagles Minimum Essential Medium) were purchased from ATCC, USA. When the cells become confluent, they were seeded on the scaffold surface at a density of 2.5×10^4 cells/sample. The scaffolds were moved to a new 24-well plate after an adhesion period of 12 hours. The culture was kept at 37°C under a 5% CO_2 atmosphere in an incubator, as recommended by the company.

The osteoblast cell (hFOB) and osteoblast growth medium were purchased from PromoCell GmbH, Germany. 3D printed scaffolds loaded with soy isoflavones were placed in 24-well plates and cells were seeded onto the scaffolds at a density of 2×10^4 cells/sample. The culture was kept in an incubator at 34°C under an atmosphere of 5% CO_2 as suggested by PromoCell for this specific cell line. For both the cultures, cell media was changed every 2–3 days during the entire cell culture.

2.4 Bioreactor Culture

All tubing, chambers, sample holders and samples were autoclaved prior to the culture at 121 °C for 60 min. The flow perfusion bioreactor is an adaption of the system illustrated by Bancroft et al. [27]. The bioreactor contains 12 separate polycarbonate flow chambers each supplied by cell media from a common media reservoir using a peristaltic pump (Cole Parmer Masterflex, Vernon Hills, IL) at a flow rate of 0.7 mL/min. Cells were seeded onto samples at a density of 1×10^6 cells/sample and kept in static culture system for 24 hours. After 24 hours, the samples were moved to the bioreactor system. The system was kept in an incubator at 34°C and a 5% CO_2 atmosphere was maintained through the entire culture. The cell media reservoir was replaced once every week.

2.5 MTT cell viability assay and cellular morphology

MTT cell viability assay (Sigma, St. Louis, MO) was carried out at 3, 7 and 11 days of cell culture. Briefly, MTT solution is prepared by dissolving MTT reagent (3-(4,5-dimethylthiazol-2-yl)-2,5-diphenyl tetrazolium bromide) in sterile-filtered Phosphate Buffered Saline (PBS) at a concentration of 5 mg/ml. 100 μl of MTT solution and 900 μl of cell media was added on top of each scaffold and incubated for 2 hours. Next, 600 μl of MTT solubilizer (10% Triton X-100, 0.1 N HCl and isopropanol) was added on the samples to dissolve the formazan crystals. After that, 100 μl of the resultant suspension was pipetted

to a new 96-well plate and optical density was measured using a microplate reader at 570 nm. To determine cytotoxicity for the osteosarcoma cell line, the percentage cell viability was calculated using the following equation:

$$\text{Cell viability (\%)} = \frac{\text{Mean value of the measured optical density of test sample}}{\text{Mean value of the measured optical density of the control}} \times 100$$

For cellular morphology by Field Emission Scanning Electron Microscopy (FESEM), samples were fixed using 2% paraformaldehyde/2% glutaraldehyde in 0.1 M phosphate buffer overnight at 4°C. Subsequently, post-fixation was carried out using 2% osmium tetroxide (OsO_4) for 1 hour at room temperature. Then, the samples were rinsed with fresh buffer solution three times followed by a dehydration procedure using a series of ethanol concentrations (30%, 50%, 70%, 95%, and 100% ethanol). In each step, samples were kept in the ethanol solution for 10–15 min. fter the ethanol dehydration, the samples were left overnight with hexamethyldisilane (HMDS) for drying. Afterward, a 10–15 nm thick gold coating was applied on the ceramic sample surface using a gold sputter coater. Finally, FESEM (FEI 200F, FEI Inc., OR, USA) was carried out to characterize the cellular morphology on the sample surface.

2.6 Alkaline phosphatase (ALP) osteoblast cell differentiation assay

ALP assay (SensoLyte® pNPP Alkaline Phosphatase Assay Kit, AnaSpec, CA, USA) was carried out to evaluate osteoblastic differentiation at 11 days of cell culture. The samples were washed twice using a 1X assay buffer. Then, 20 μl of Triton X-100 was added to 10 mL of 1X assay buffer and this solution was added on top of the samples. The adherent cells were scraped off and the collected cell suspension was incubated at 4°C for 10 min. Then, the suspension was subjected to centrifugation at 2500 g for 10 min at 4°C. The resultant supernatant was collected for ALP assay and transferred to a 96-well plate. 50 μL of *p*NPP substrate solution was added followed by mixing the reagents by gently shaking the plate for 30 sec. The reaction was incubated for 45 min at room temperature. Finally, 50 μL of stop solution was added into each well. The plate is shaken on a plate shaker for a minute before measuring the absorbance at 405 nm wavelength in a microplate reader. The ALP/cell has been expressed by normalizing with the viable cell number from MTT assay (OD_{405}/OD_{570}).

2.7 Surgery and implantation procedure

The *in vivo* surgeries and experimental procedure were approved by the Institutional Animal Care and Use Committee (IACUC), Washington State University. The subjects were male Sprague-Dawley rats (Envigo, IN, USA) with a bodyweight of 280–320g. Upon arrival, the rats were kept in a standard condition (room temperature of 20°*C*, and normal humidity) and given regular food and water. Prior to the surgery, the rats were anesthetized with IsoFlo® (isoflurane, USP, Abbott Laboratories, North Chicago, IL, USA) along with oxygen (Oxygen USP, A-L Compressed Gases Inc., Spokane, WA, USA). Pedal reflex and respiration rate of the rats were monitored to maintain proper surgical anesthesia. Surgery was performed to generate a critical sized bi-cortical defect (3–5 mm) in the lateral epicondyle by means of sterile drill bits (1–3 mm, step 0.5 mm). Physiological saline was

used to rinse the cavity during drilling to prevent thermal necrosis and remove small bone fragments present. Thereafter, soy isoflavone loaded 3D printed TCP scaffolds were placed at the created defect site. The wound was closed by suturing with an absorbable synthetic surgical suture, undyed 4–0 MONOCRYL (Ethicon Inc., Somerville, NJ, USA). 3 mls of subcutaneous saline was given after the surgery. Buprenorphine subcutaneous injection was given as a pre- and post-operative pain-relieving aid. Rats were sacrificed 24 hours after implantation by CO_2 overdose. The bone tissue-implant sections were separated from the rat and fixed with 10% neutral buffered formalin solution for 72 hours.

2.8 Histomorphology of decalcified tissue sections by Hematoxylin & Eosin (H&E) staining

The formalin-fixed tissue samples were washed with deionized (DI) water 2–3 times and then kept in 5% formic acid for at least 24 hours for decalcification. The decalcification endpoint was checked by submerging the decal solution in a combination of ammonium hydroxide and ammonium oxalate. When the specimen is completely decalcified, the test aliquot was clear and colorless. After rinsing the specimen with DI water, the bone samples were embedded in paraffin and cut into 5–15 μm thin section. The section was deparaffinized and rehydrated in a series of xylene, ethanol (100%, 95%, and 70%) followed by washing in DI water. Finally, H&E staining was carried out and stained section was imaged in an optical microscope (Leica Microsystems, IL, USA).

2.9 Statistical Analyses

All experimental data are representative of three biological replicates (n=3) and three technical replicates. The data were normally distributed by the Shapiro–Wilk test and are represented as mean±SD. Statistical analyses were performed in GraphPad Prism 8 software (CA, USA) using two-way ANOVA and Bonferroni post-hoc analysis. P values ≤ 0.05 were considered as statistically significant. The software analysis, procedure and *in vivo* quantitative data analysis is described elsewhere. [34]

3. Results

3.1 3D printed scaffold: design and architecture

Fig. 1 shows software generated CAD file with designed interconnected pores with a size of 400 m. The FESEM image of the sintered scaffold exhibits the macropore size ranging from 342–350 μm and micropores in the range of 5–20 μm.

3.2 *In vitro* soy isoflavones release from 3D printed scaffold

Fig. 2 show *in vitro* release profiles of genistein, daidzein and glycitein from 3DP TCP scaffold in independent and combination form at pH 7.4 (DMEM supplemented with 10% FBS). Fig. 2A shows the acid dissociation constant or pKa values for genistein, daidzein and glycitein are 6.51, 6.48 and 6.92, indicating that these isoflavones are easily deprotonated at physiological pH of 7.4. The release data depicted in the fig. 2(B-D) shows long term sustained release for all three isoflavones at pH 7.4. When all three isoflavones are loaded in 5:4:1 ratio, 72.52% release of genistein was achieved in 16 days (Fig. 2B), whereas daidzein accounted for 100% release during the same time period (Fig. 2C). Glycitein showed an

overall lower release of 13.75% from the combined form. Moreover, the individual release of the drugs was also carried out to understand the effect of one drug on the release of the other. Genistein, daidzein and glycitein showed independent release behaviors with 69.87, 77.69% and 14.65% release, respectively, in pH 7.4 buffer media.

In an acidic buffer solution, the drugs followed a slower release trend, while genistein, daidzein and glycitein individually released 25.37, 16.97 and 3.44% respectively, as shown in Fig. 3. Meanwhile, the isoflavones at 5:4:1 ratio in the combined delivery system showed 19.02, 23.87 and 2.97% of release after 16 days by genistein, daidzein, and glycitein respectively. Notably, daidzein showed a significantly enhanced drug release when formulated in a combination form (5:4:1), unlike the other two isoflavones genistein and glycitein, who showed comparatively lower release in combination form.

3.3 Osteosarcoma cell culture: assessment of *in vitro* chemopreventive properties of scaffold

Chemopreventive effect of soy isoflavones was assessed in osteosarcoma (MG-63) cell line with MTT assay at day 3, 7 and 11, as shown in Fig. 4. Results showed that genistein exhibited the lowest cell viability compared to the control and other treatments at all time points. Percentage cell viability in table 1 shows 33, 14 and 4% of cell viability at day 3, 7 and 11 respectively in the presence of genistein. Daidzein and glycitein exhibited only limited cytotoxicity at day 3 and day 7 with cell viability as 55% and 66% at day 3 and 94% and 61% at day 7. However, genistein-induced chemoprevention resulted in significantly higher osteosarcoma toxicity in the presence of all three isoflavones. Genistein, daidzein, and glycitein in a ratio of 5:4:1 showed 90% lower MG-63 cellular proliferation at day 11 compared to the control, implying its potential chemopreventive effects towards osteosarcoma cell line.

FESEM was carried out to evaluate the effect of soy isoflavones on the morphology and proliferation of osteosarcoma cell line at day 3, 7 and 11, shown in Fig. 5. Control 3DP TCP scaffold shows layers of osteosarcoma attachment due to the presence of a large number of proliferating cells at all the time points. Genistein showed very few to almost no presence of osteosarcoma cell attachment in comparison to control. Daidzein and glycitein showed limited sensitivity towards osteosarcoma cells, however, three isoflavones together showed very few proliferating cells due to the presence of genistein in the system.

3.4 Assessment of *in vitro* cytocompatibility of scaffold

3.4.1 Scaffold promotes osteoblast cell proliferation in static condition—

Since the presence of genistein exhibited higher toxicity in osteosarcoma cell lines, its effect was further evaluated in a human fetal osteoblast cell line (hFOB), as shown in Fig. 6. The result showed the effect of genistein on hFOB was minimal, implying its non-cytotoxicity towards normal cells. However, daidzein exhibited significant cellular viability towards the hFOB cell line ($p<0.001$), compared to control. Glycitein did not show much proliferating effects on hFOB cell viability ($p>0.05$), however it did not possess any cytotoxicity either. Additionally, the presence of three isoflavones showed the highest cell viability with an almost eight-fold greater hFOB cell density at day 11 ($p<0.001$).

To investigate the effect of soy isoflavones on hFOB cellular morphology and proliferation, FESEM was carried out at day 3, 7 and 11, as shown in Fig. 7. Genistein showed a scarce amount of osteoblast cells on day 7 and 11, compared to control. However, daidzein showed a distinct hFOB cellular morphology with an extensive amount of filopodial extension as compared to the control. The filopodial extensions act as an anchor and aid in further cellular attachment and extension. Glycitein showed very few osteoblast attachments at day 3 and 7, which comparatively enhanced at day 11. Additionally, genistein, daidzein, and glycitein exhibited deposition of mineralized particles onto a thick layer of osteoblast cells covering the entire sample surface.

3.4.2 Scaffold promotes osteoblast cell proliferation and differentiation in dynamic condition—

hFOB cells were cultured on soy isoflavones loaded 3DP TCP scaffolds in a static condition and were moved to a flow perfusion bioreactor after 24 hours. The schematic diagram of flow perfusion bioreactor is shown in Fig. 8A–B. MTT assay showed that the presence of soy isoflavones exhibited an almost one-fold increase in cellular viability at day 5, as shown in Fig. 8C. The cellular viability doubled from day 5 to day 10, in the presence of soy isoflavones. The ALP assay at day 10, showed a higher normalized ALP density for soy isoflavones loaded 3DP TCP scaffold in comparison to the control, implying its possible effect in hFOB differentiation.

hFOB cell attachment and growth on control and soy isoflavone loaded samples were analyzed by FESEM, as shown in Fig. 9. In terms of cell attachment, hFOB seeded on soy isoflavones loaded samples, shows higher growth and firm attachment with complex filopodial extensions compared to control. Control samples show the presence of hFOB, however with reduced proliferation and weaker attachment. It is interesting to note that the cells are seen accumulated near the porous regions of the scaffold, suggesting the importance of nutrient transport in the dynamic cell culture system.

3.5 In vivo study: assessment of inflammatory responses in rat distal femur model

Next, in order to examine the *in vivo* inflammatory responses, soy isoflavone-loaded 3DP TCP scaffold was implanted in a rat distal femur critical-sized defect model. The animals were sacrificed after 24 hours and the inflamed site was examined for inflammatory factors using H&E staining, as shown in Fig. 10. Notably, genistein showed efficacy by showing fewer neutrophil recruitment at the implant site. Presence of all three isoflavones at 5:4:1 ratio showed evidence of immunomodulatory responses by exhibiting controlled neutrophil recruitment surrounding the implants.

Based on H&E staining, a quantitative measurement was carried out to represent neutrophils recruitment table 2. Control shows higher inflammatory cell recruitment, whereas, presence of genistein and soy isoflavones, markedly reduced neutrophils recruitment. The scatter plots in Fig. 11 were obtained from 10 bone-tissue sections, which exhibited significant signs of modulated inflammatory reactions in presence of genistein and soy isoflavones, compared to the control ($p<0.001$).

4 Discussion

The self-reconstruction ability of bone fails to perform in the cases of critical-sized bone defects, such as those associated with bone tumor resection. Surgical resection is the primary mode of treatment for bone malignancies; however, it often leaves residual malignant cells which migrate to other tissues or organs and tend to reappear within a few years. A localized drug delivery approach, which incorporates both chemopreventive and osteogenic agents into a biodegradable porous scaffold may represent a key solution to the recent challenges in post-surgical bone cancer management. [35] This study, for the first time, documents the delivery of three primary soy isoflavones with significantly improved *in vitro* chemopreventive and osteogenic properties from bioresorbable porous TCP scaffolds, prepared by a binder-jet 3D printing process.

Owing to its high interconnected porosity, 3D printed bone tissue engineering scaffolds with designed microarchitecture demonstrates enhanced cell seeding, cell migration through guided channels and higher bone tissue regeneration. [36–38] Multimodal porosity is one of the most important requirements of designed scaffolds,[39] which includes macropores (50–300 μm) for tissue ingrowth and cell attachment, and micropores (2–50 μm) for nutrient and metabolic waste transport. Based on these literary data, we have designed a CAD file with a designed pore size of 400 μm, which resulted in a sintered pore size of 346±5 μm. A maximum compressive strength of about 4.9±0.7 MPa has been recorded for these scaffolds, which is in compliance with the mechanical strength of human trabecular bone (0.22–10.44 MPa) [40–42]. Homogeneously distributed micropores with a size range of 5–20μm can also be observed in the scaffold strut. For drug-loaded scaffold, these micropores also assist in diffusion-based drug release. In addition to the porosity, the scaffold degradation rate is another important parameter which contributes to the desired release of the loaded drug. While choosing an appropriate bioceramic for 3D printed scaffold, its dissolution rate needs to be considered for the above reasons. TCP ceramics have exhibited a better biodegradability compared to other biomaterials, including hydroxyapatite, due to its faster degradation rate. It also releases calcium and phosphate ions *in vitro* and *in vivo*, thus forming a biological apatite precipitate on scaffold surface which leads to a strong bone bonded surface. These 3D printed TCP scaffolds are capable of providing a microenvironment for cell attachment, proliferation, distribution, and differentiation, establishing its potential to assist in bone regeneration. [43]

After a successful fabrication of 3D printed TCP scaffolds with osteoconductive properties, their efficacy in drug delivery and cell attachment was evaluated. The *in vitro* release study was performed in DMEM (pH 7.4) and acetate buffer (pH 5.0) to simulate the physiological and post-surgical microenvironment. Ideally, local delivery of chemopreventive drugs should exhibit a higher initial release to combat the residual bone cancer cells in the surrounding tissue sections, followed by a sustained release at an effective level to prevent the recurrence of the tumor. In the case of the osteogenic drug, an initial burst release can improve the wound healing time and a sustained release of effective drug concentration can promote new bone regeneration as the scaffold degrades over time. Our results showed, all three isoflavones, genistein, daidzein, and glycitein exhibited an initial burst release in first 72 hours (about 40% and 15% in pH 7.4 and 5.0, respectively) followed by a sustained release

for at least 16 days. Surgery and implantation create an acidic microenvironment at the defect site, which persists for almost two weeks before it returns to the normal physiological pH. In pH 5.0, the isoflavones showed almost 20% release in the first two weeks, promising drug delivery potential in a post-implantation defect site. To represent the physiological environment, Dulbecco's Modified Eagle medium (DMEM) solution have been used in this study as one of the release media for *in vitro* drug release kinetics evaluation. DMEM supplemented with FBS contains components from blood serum, and organic constituents such as vitamins, amino acids, and proteins, which helps to better simulate the *in vivo* environment of a living body, compared to the SBF (simulated body fluid) or PBS (phosphate buffer solution) containing only inorganic components. These proteins and amino acids are readily absorbed on the calcium phosphate scaffold surface and result in the higher surface activity and subsequent dissolution of Ca^{2+} and PO_4^{3-}[44]. It is also likely that the presence of 10% FBS caused the formation of drug-protein complex, and an enhancement of drug solubility in release media, which might be an explanation for observing an overall higher release of all drugs in pH 7.4, compared to the pH 5.0 or acetate buffer solution. Moreover, it is interesting to note that the acid dissociation constant or pKa values for genistein, daidzein and glycitein are 6.51, 6.48 and 6.92, indicating that these isoflavones are easily deprotonated at physiological pH of 7.4, whereas at pH 5.0, they primarily stay in partially protonated form resulting in lower solubility. Genistein is stabilized by two mechanisms; primarily due to the hydrogen bonding between C(4) carbonyl oxygen and C(5) -OH group to maintain the lowest-minimum energy state. Besides, it forms a resonance stabilization structure allowing delocalization of unpaired electrons within C(4) carbonyl oxygen and C(5) -OH group. In case of daidzein and glycitein, the first pKa for daidzein and glycitein are because of their ability to generate phenoxyl radical by donating the most easily abstractable hydrogen from C(7)-OH group [45]. Furthermore, the results demonstrated that the individual drug releases in case of daidzein, and genistein are lesser than the combined release system, which implies that the drugs did not affect each other's release. Moreover, due to an almost identical chemical structure, genistein, daidzein and glycitein act synergistically when incorporated together. Genistein is known to be less stable in acidic pH, and lower genistein release at pH 5.0, when administered in combination form, might be attributed to degradation or conversation into other unknown isoflavone derivatives that were undetectable by the UV-vis protocol used [46]. Glycitein's lower release in combination form can be easily explained by its overall lower percentage (10%) in the drug formulation compared to that of genistein (50%) or daidzein (40%), together which may have subdued the release of glycitein. Besides, all the cumulative release kinetics for genistein, daidzein and glycitein are best fitted with the Korsmeyer-Peppas model, which is characteristic drug release kinetics for cylindrical drug delivery system.

Following a controlled drug release of soy isoflavones from the 3D printed TCP scaffolds, the *in vitro* cytotoxicity study was carried out utilizing osteosarcoma (MG-63) cell line. The results showed a significant decrease in MG-63 cell viability and proliferation ($p<0.0001$) in the presence of genistein at day 3, 7 and 11, compared to control. Notably, less than 95% of osteosarcoma cellular viability is observed at day 11 by genistein. Although daidzein and glycitein individually showed minimum sensitivity towards MG-63 cell, all three isoflavones

together showed significant cellular toxicity ($p<0.0001$) suggesting the chemopreventive efficacy of genistein in the combination. It is worth mentioning that based on ISO 10993–5 guideline[47], cellular viability of less than 70% suggests that the biomolecule has the potential for use as a chemopreventive agent. These results are validated by early *in vitro* and *in vivo* reports which show genistein potentially act as a chemopreventive agent against different types of cancers including hormone-dependent breast and prostate tumor as well as non-hormone-dependent cancers such as colon, gastric, lung, and pancreatic tumors. [7–12] One of the mechanisms suggests that isoflavones inhibits the activation of NF-κB, which is a transcription factor involved in inflammatory responses and balance between cell survival and programmed cell death (Fig. 13A). [48] NF- $\kappa\beta$ are present in cytoplasm conjugated with its inhibitor (I$\kappa\beta$), which keeps it in inactivated state. In malignant cells, presence of various cytokines, oncogenic stress, ROS results in phosphorylation and subsequent degradation of I$\kappa\beta$, followed by the release and activation of free NF-$\kappa\beta$. [49] Activated NF-$\kappa\beta$ travels to nucleus and contributes to the development of various malignant disorders. Soy isoflavones inhibit the phosphorylation and degradation of I$\kappa\beta$, which keeps NF-$\kappa\beta$ in its inactivated state in cytoplasm and thereby exhibits selective cytotoxicity towards malignant cells (Fig. 13A).

After evaluating the potential *in vitro* chemopreventive properties against MG-63 cells, it is necessary to monitor their biological safety towards normal bone cells (hFOB). The isoflavones did not exert any toxicity towards the hFOB cells, in fact, daidzein showed improved cellular viability in day 3, 7 and 11. Presence of daidzein demonstrated a firm attachment of hFOB cells and formation of filopodial extensions on the scaffold surface, however combination of three isoflavones demonstrated the highest MTT cell metabolic activity compared to the individual drugs. This can be explained by the drug release kinetics in DMEM, where the cumulative drug release was significantly higher when three drugs are incorporated together, compared to the sum of individual drug release. Higher released drug might be able to exert improved osteoblast cellular activity. The osteogenic ability of soy isoflavones have demonstrated to be mediated through the estrogen receptor (ER) dependent pathways, primarily through ER-β. Due to their structural similarity with the estrogen, isoflavones can bind to the estrogen receptors, ERα and ERβ which are also present in osteoblastic cells. For an instance, genistein exhibits 4% and 87% binding affinity towards ER and ERβ, respectively, compared to that of estradiol. The selective binding of genistein to ERβ mimics the estrogenic activity in bone tissues by maintaining the bone mineral density, while the estrogen-antagonistic activity of ERβ reduce the risk of hormone-related cancer by exhibiting anti-proliferative effects (Fig. 13B). [50] Although daidzein shows much less affinity towards ERα and ERβ, it is reported to increase osteoprotegerin (OPG) secretion by osteoblast lineage cells and significantly decrease expression of NF-κB. A decrease in NF-κB expression inhibits the RANKL/RANK pathway which prevents osteoclast maturation and differentiation from preosteoclasts (Fig. 13C. [51–52] The selective toxicity of soy isoflavones can be demonstrated by the NF-κB pathway. The transcription factor NF-κB is only activated in osteosarcoma cells in response to diverse stress and inflammatory stimuli and mediates cellular interpretation of the triggering stimuli via regulation of gene expression. Soy isoflavones downregulates NF-κB activation in osteosarcoma cells and therefore arrests MG-63 cell proliferation and viability. On the other

hand, isoflavones induces osteoblast proliferation due to their structural similarity to the estrogen and subsequently binding to the estrogen receptor.

This study also addresses a fundamental issue in tissue engineering, in particular, regarding the effects of dynamic flow-induced nutrient transport on *in vitro* bone cell proliferation. A flow perfusion bioreactor has been designed and built in our lab which fulfills the following requirements: i) deliver the flow through the scaffold, ii) allow a repeatable, controllable, and consistent rate of flow delivered to the scaffold, iii) can be sterilized and sterile conditions can be maintained throughout the culture period. After 5 days of dynamic culture, soy isoflavones have demonstrated enhanced cellular proliferation ($p<0.05$) compared to the control, which is in line with the static culture. Conversely, at 10 days, higher osteoblast cell proliferation is noted in case of control sample. This unique phenomenon can be explained with the help of figure 4D, where we can see the proliferated and matured hFOB cells in presence of soy isoflavones have started differentiating at day 10 suggesting their faster proliferation rate compared to the control. On the other hand, control scaffolds show much lesser osteoblast cell differentiation ($p<0.05$) at day 10 compared to soy isoflavones. This can be attributed to the presence of immature osteoblast cells in control scaffolds, which were still proliferating at day 10, resulting in higher viability during that time compared to the soy isoflavones loaded scaffolds. Furthermore, comparatively more cells were present in the interior of the scaffolds and pores under dynamic conditions than that of static culture. This is attributed to the dynamic flow which improves nutrient supply and waste product removal and thus promotes cellular growth in the scaffold interior. [53]

After investigating the effect of soy isoflavones on osteoblast and osteosarcoma cellular activity, we were also interested to explore its ability to modulate post-surgical acute inflammation. The process of postoperative bone healing involves the recruitment of monocytes/neutrophils, the inflammatory cells that are associated with the innate immune system. [54] Following implantation, neutrophils are the first immune cells to be recruited in the injury site and lead the host defense reaction to tissue damage. Upon arriving, they destroy foreign pathogens and minimize tissue damage by several mechanisms. However, excess infiltration and activation of neutrophils causes chronic inflammation, limit injury repair and implant rejection. Therefore, the emerging view is that the inflammation is a key for efficient tissue regeneration and repair, however it needs to be finely controlled or modulated to ensure early wound healing and subsequent defect repair. [55–56] As a preliminary step to evaluate immunomodulatory activity *in vivo*, soy isoflavones loaded 3DP TCP scaffolds were implanted on a 3/5 mm epicondyle defect in rat distal femur model. Increased density of neutrophils was observed around the implant site of control samples, indicating a major sign of acute inflammation. However, the presence of genistein and combination of soy isoflavones controlled neutrophil recruitment at the surgery site. These preliminary findings suggest the efficacy of soy isoflavones towards the modulation of postoperative acute inflammation, which is also in line with the previous reports of anti-inflammatory activity of genistein and daidzein.[19–22] Together, the results from the present study indicate the soy isoflavone loaded 3D printed scaffold exhibits a multifunctional ability of *in vitro* chemopreventive effect against MG-63 cells and enhanced osteoblast cell proliferation, viability, differentiation, in both static and dynamic system.

Our study is not beyond limitations. Other malignant cell lines like SAOS-2, HOS-MNNG, K-HOS and MOS-J need to be further tested against soy isoflavones-incorporated bone scaffolds to confirm their broadspread chemopreventive efficacy for post-tumor resection defect repair application. Another limitation of this study is insufficient characterizations based on the expression of bone markers such as RunX-2, OCN, OPN and BSP, which need to be addressed in future work. Lastly, the *in vivo* study presented in this paper is in its preliminary stage. Therefore, further long-term studies should be performed, as well as the effect of these isoflavones on *in vitro* neutrophil response need to be carried out.

5 Summary

A multifunctional scaffold was fabricated by incorporating soy isoflavones, genistein, daidzein, and glycitein in 5:4:1 ratio, mimicking their original proportion in soy isoflavones, onto a 3D printed TCP scaffold with designed porosity. The 3D printed scaffold possesses multimodal porosity, which includes designed macropores in the size range of 400 μm, whereas intrinsic residual micropores of 5–20 μm can be observed in the scaffold strut. The interconnected porosity and biodegradability of TCP ceramics allowed a controlled and sustained release three major isoflavones, genistein, daidzein and glycitein. In physiological pH, genistein, daidzein and glycitein exhibited 72.5, 100 and 13.75% release, respectively, whereas, in acidic pH, 25.1, 23.3 and 2.97% release were observed by genistein and daidzein, respectively, after 16 days. *In vitro* chemopreventive potential of genistein was assessed individually and in the presence of daidzein and glycitein, which shows 90% reduction in cellular viability after 11 days, compared to control. *In vitro* osteoblast cell culture was carried out in both static and dynamic condition to ensure the biological safety of isoflavones towards normal bone cells. Daidzein showed enhanced hFOB cellular activity, by improving its growth, attachment, and proliferation as compared to control. Meanwhile, the *in vitro* hFOB cell culture was carried out in a flow perfusion bioreactor, which better mimics the clinical environment compared to the static culture. The soy isoflavones loaded 3D printed scaffolds showed increased cellular viability, proliferation, and differentiation ($p<0.0001$), compared to the control at day 5 and 10. Finally, neutrophil recruitment at the inflammation site was demonstrated using H&E staining suggesting the immunomodulatory potential of soy isoflavones at 24 hours post-surgical specimens from rat distal femur model.

Supplementary Material

Refer to Web version on PubMed Central for supplementary material.

Acknowledgment

Authors would like to acknowledge financial support from the National Institutes of Health under grant number R01 AR066361. The content is solely the responsibility of the authors and does not necessarily represent the official views of the National Institute of Health.

References

1. Durfee RA, Mohammed M, Luu HH, Review of osteosarcoma and current management. Rheumatol Ther. 3 (2016) 221–243. 10.1007/s40744-016-0046-y [PubMed: 27761754]

2. Croucher PI, McDonald MM, Martin TJ, Bone metastasis: the importance of the neighbourhood, Nat. Rev. Cancer 16 (2016) 373. 10.1038/nrc.2016.44. [PubMed: 27220481]

3. Winkler T, Sass FA, Duda GN, & Schmidt-Bleek K (2018). A review of biomaterials in bone defect healing, remaining shortcomings and future opportunities for bone tissue engineering: The unsolved challenge. Bone & joint research, 7(3), 232–243. doi: 10.1302/2046-3758.73.BJR-2017-0270.R1 [PubMed: 29922441]

4. Fernandez de Grado G, Keller L, Idoux-Gillet Y, Wagner Q, Musset AM, Benkirane-Jessel N, ... & Offner D (2018). Bone substitutes: a review of their characteristics, clinical use, and perspectives for large bone defects management. Journal of tissue engineering, 9, 2041731418776819. doi: 10.1177/2041731418776819.

5. Bose S, Tarafder S, & Bandyopadhyay A (2017). Effect of chemistry on osteogenesis and angiogenesis towards bone tissue engineering using 3D printed scaffolds. Annals of biomedical engineering, 45(1), 261–272. 10.1016/j.biomaterials.2007.06.023 [PubMed: 27287311]

6. Bose S, Sarkar N, Banerjee D, Effects of PCL, PEG and PLGA polymers on curcumin release from calcium phosphate matrix for in vitro and in vivo bone regeneration, Mater. Today Chem 8 (2018) 110–120. 10.1016/j.mtchem.2018.03.005 [PubMed: 30480167]

7. Ginebra MP, Canal C, Espanol M, Pastorino D, Montufar EB, Calcium phosphate cements as drug delivery materials. Advanced drug delivery reviews, 64 (2012) 1090–1110. 10.1016/j.addr.2012.01.008 [PubMed: 22310160]

8. Bose S, Vahabzadeh S, & Bandyopadhyay A (2013). Bone tissue engineering using 3D printing. Materials today, 16(12), 496–504. 10.1016/j.mattod.2013.11.017

9. Sarkar N, Bose S, Liposome-encapsulated Curcumin Loaded 3D Printed Scaffold for Bone Tissue Engineering, ACS Appl. Mater. Interfaces 11 (2019) 17184–17192. 10.1021/acsami.9b01218. [PubMed: 30924639]

10. Simoons FJ, Food in China: a cultural and historical inquiry, CRC Press, 2014. 10.1201/9781482259322

11. Setchell KD, Phytoestrogens: the biochemistry, physiology, and implications for human health of soy isoflavones, Am. J. Clin. Nutr 68 (1998) 1333S–1346S. 10.1093/ajcn/68.6.1333S. [PubMed: 9848496]

12. Kalaiselvan V, Kalaivani M, Vijayakumar A, Sureshkumar K, Venkateskumar K, Current knowledge and future direction of research on soy isoflavones as a therapeutic agents. Pharmacogn. Rev 4 (2010) 111. 10.4103/0973-7847.70900. [PubMed: 22228950]

13. Kuiper, George GJM, Lemmen JG, Carlsson BO, Corton JC, Safe SH, an er Saag PT, an er Burg B, . .Gustafsson, nteraction of estrogenic chemicals and phytoestrogens with estrogen receptor β, Endocrinology. 139 (1998) 4252–4263. 10.1210/endo.139.10.6216 [PubMed: 9751507]

14. Clarkson TB, Soy, soy phytoestrogens and cardiovascular disease, J. nutr 132 (2002) 566S–569S. 10.1093/jn/132.3.566S [PubMed: 11880594]

15. Velasquez MT, Bhathena SJ, Role of dietary soy protein in obesity, Int. J. Med. Sci 4 (2007) 72. 10.7150/ijms.4.72 [PubMed: 17396158]

16. Wu AH, Yu MC, Tseng CC, Pike MC, Epidemiology of soy exposures and breast cancer risk, Br. J. Cancer 98 (2008) 9. 10.1038/sj.bjc.6604145 [PubMed: 18182974]

17. Applegate C, Rowles J, Ranard K, Jeon S, Erdman J, Soy consumption and the risk of prostate cancer: An updated systematic review and meta-analysis, Nutrients 10 (2018) 40. 10.3390/nu10010040.

18. Banerjee S, Li Y, Wang Z, Sarkar FH, Multi-targeted therapy of cancer by genistein, Cancer Lett. 269 (2008) 226–242. 10.1016/j.canlet.2008.03.052. [PubMed: 18492603]

19. Pons DG, Nadal-Serrano M, Torrens-Mas M, . Oliver P. Roca, The phytoestrogen genisteinaffects breast cancer cells treatment depending on the ERα/ERβ ratio, . Cell. Biochem 117 (2016) 218–229. 10.1002/jcb.25268.

20. Zhang Z, Jin F, Lian X, Li M, Wang G, Lan B, He H, Liu GD, Wu Y, Sun G, Xu CX, Genistein promotes ionizing radiation-induced cell death by reducing cytoplasmic Bcl-xL levels in non-small cell lung cancer, Sci. Rep 8 (2018) 328. 10.1038/s41598-017-18755-3 [PubMed: 29321496]

21. Spagnuolo C, Russo GL, Orhan IE, Habtemariam S, Daglia M, Sureda A, Nabavi SF, Devi KP, Loizzo MR, Tundis R, Nabavi SM, Genistein and cancer: current status, challenges, and future directions.Adv. Nutr 6 (2015) 408–419. 10.3945/an.114.008052. [PubMed: 26178025]
22. Hirata H, Hinoda Y, Shahryari V, Deng G, Tanaka Y, Tabatabai ZL, Dahiya R, Correction: Genistein downregulates onco-miR-1260b and upregulates sFRP1 and Smad4 via demethylation and histone modification in prostate cancer cells, Br. J. Cancer 119 (2018) 388. 10.1038/s41416-018-0146-2. [PubMed: 29930252]
23. Pavese JM, Farmer RL, Bergan RC, Inhibition of cancer cell invasion and metastasis by genistein, Cancer Metastasis Rev. 29 (2010) 465–482. 10.1007/s10555-010-9238-z. [PubMed: 20730632]
24. Picherit C, Coxam V, Pelissero CB, Kati-Coulibaly S, Davicco MJ, Lebecque P, Barlet JP, Daidzein is more efficient than genistein in preventing ovariectomy-induced bone loss in rats., J. Nutr 130 (2000) 1675–1681.10.1093/jn/130.7.1675 [PubMed: 10867035]
25. Jia TL, Wang HZ, Xie LP, Wang XY, Zhang RQ, Daidzein enhances osteoblast growth that may be mediated by increased bone morphogenetic protein (BMP) production, Biochem. Pharmacol 65 (2003) 709–715. 10.1016/s0006-2952(02)01585-x [PubMed: 12628484]
26. Smith BN, & Dilger RN (2018). Immunomodulatory potential of dietary soybean-derived isoflavones and saponins in pigs. Journal of animal science, 96(4), 1288–1304. 10.1093/jas/sky036 [PubMed: 29471443]
27. Mace TA, Ware MB, King SA, Loftus S, Farren MR, McMichael E, ... & Clinton SK (2019). Soy isoflavones and their metabolites modulate cytokine-induced natural killer cell function. Scientific reports, 9(1), 1–12. 10.1038/s41598-019-41687-z [PubMed: 30626917]
28. Li HY, Pan L, Ke YS, Batnasan E, Jin XQ, Liu ZY, Ba XQ, Daidzein suppresses pro-inflammatory chemokine Cxcl2 transcription in TNF-α-stimulated murine lung epithelial cells via depressing PARP-1 activity. Acta Pharmacol. Sin 35.4 (2014): 496. 10.1038/aps.2013.191 [PubMed: 24632845]
29. Han S, Wu H, Li W, Gao P, Protective effects of genistein in homocysteine-induced endothelial cell inflammatory injury, Mol. Cell. Biochem 403 (2015), 43–49 10.1007/s11010-015-2335-0. [PubMed: 25626894]
30. Yu J, Bi X, Yu B, Chen D, Isoflavones: anti-inflammatory benefit and possible caveats, Nutrients 8 (2016) 361. 10.3390/nu8060361.
31. Selden C, Fuller B, Role of bioreactor technology in tissue engineering for clinical use and therapeutic target design, Bioengineering 5 (2018) 32. 10.3390/bioengineering5020032.
32. Bancroft GN, Sikavitsas VI, Mikos AG, Design of a flow perfusion bioreactor system for bone tissue-engineering applications. Tissue engineering 9 (2003) 549–554. 10.1089/107632703322066723 [PubMed: 12857422]
33. Cartmell SH, Porter BD, García AJ, Guldberg RE, Effects of medium perfusion rate on cell-seeded three-dimensional bone constructs in vitro. Tissue engineering 9 (2003) 1197–1203. 10.1089/10763270360728107 [PubMed: 14670107]
34. Soltzberg J, Frischmann S, van Heeckeren C, Brown N, Caplan A, & Bonfield TL (2011). Quantitative microscopy in murine models of lung inflammation. Analytical and quantitative cytology and histology/the International Academy of Cytology [and] American Society of Cytology, 33(5), 245.
35. Bose S, & Sarkar N (2019). Natural Medicinal Compounds in Bone Tissue Engineering. Trends in Biotechnology. 10.1016/j.tibtech.2019.11.005
36. Tarafder S, Balla K, avies NM, Bandyopadhyay A, & Bose S (2013). Microwave-sintered 3D printed tricalcium phosphate scaffolds for bone tissue engineering. Journal of tissue engineering and regenerative medicine, 7(8), 631–641. 10.1002/term.555 [PubMed: 22396130]
37. Won JE, Lee YS, Park JH, Lee JH, Shin YS, Kim CH, ... & Kim HW (2020). Hierarchical microchanneled scaffolds modulate multiple tissue-regenerative processes of immune-responses, angiogenesis, and stem cell homing. Biomaterials, 227, 119548.
38. Barba A, Maazouz Y, Diez-Escudero A, Rappe K, Espanol M, Montufar EB, ... & Franch J (2018). Osteogenesis by foamed and 3D-printed nanostructured calcium phosphate scaffolds: effect of pore architecture. Acta biomaterialia, 79, 135–147. [PubMed: 30195084]

39. Porter JR, Ruckh TT, Popat KC, Bone tissue engineering: a review in bone biomimetics and drug delivery strategies. Biotechnology progress, 25 (2009) 1539–1560.10.1002/btpr.246 [PubMed: 19824042]
40. Vahabzadeh S, & Bose S (2017). Effects of iron on physical and mechanical properties, and osteoblast cell interaction in β-tricalcium phosphate. Annals of biomedical engineering, 45(3), 819–828. [PubMed: 27896489]
41. Bose S, Banerjee D, Robertson S, & Vahabzadeh S (2018). Enhanced in vivo bone and blood vessel formation by iron oxide and silica doped 3D printed tricalcium phosphate scaffolds. Annals of biomedical engineering, 46(9), 1241–1253. [PubMed: 29728785]
42. Ke D, Tarafder S, Vahabzadeh S, & Bose S (2019). Effects of MgO, ZnO, SrO, and SiO2 in tricalcium phosphate scaffolds on in vitro gene expression and in vivo osteogenesis. Materials Science and Engineering: C, 96, 10–19.
43. Mouriño V, Boccaccini AR, Bone tissue engineering therapeutics: controlled drug delivery in three-dimensional scaffolds. Journal of the Royal Society Interface, 7 (2009) 209–227. doi:10.1098/rsif.2009.0379
44. Dziadek M, Zagrajczuk B, Menaszek E, & Cholewa-Kowalska K (2018). A new insight into in vitro behaviour of poly (ε-caprolactone)/bioactive glass composites in biologically related fluids. Journal of materials science, 53(6), 3939–3958.
45. Frontiers in Natural Product Chemistry, Volume 3 edited by Atta-ur-Rahman, Bentham Science Publishers, 2017, 270–271.
46. Mathias K, Ismail B, Corvalan CM, & Hayes KD (2006). Heat and pH effects on the conjugated forms of genistin and daidzin isoflavones. Journal of Agricultural and Food Chemistry, 54(20), 7495–7502. [PubMed: 17002413]
47. International Organization for Standardization (ISO 10993–5) 2009 Biological evaluation of medical devices — Part 5: Tests for in vitro cytotoxicity. https://www.iso.org/obp/ui#iso:std:iso:10993:−5:ed-3:v1:en
48. Adjakly M, Ngollo M, Boiteux JP, Bignon YJ, Guy L, Bernard-Gallon D, Genistein and daidzein: different molecular effects on prostate cancer, Anticancer Res. 33 (2013) 39–44. PMID: 23267126 10.1073/pnas.0402532101 [PubMed: 23267126]
49. Park Mi, and Hong Jin. “Roles of NF-κB in cancer and inflammatory diseases and their therapeutic approaches.” Cells 5, no. 2 (2016): 15.
50. Ming LG, Chen KM and Xian CJ, 2013. Functions and action mechanisms of flavonoids genistein and icariin in regulating bone remodeling. Journal of cellular physiology, 228(3), pp.513–521. [PubMed: 22777826]
51. Heim M, Frank O, Kampmann G, Sochocky N, Pennimpede T, Fuchs P, Hunziker W, Weber P, Martin I, Bendik I, The phytoestrogen genistein enhances osteogenesis and represses adipogenic differentiation of human primary bone marrow stromal cells, Endocrinology. 145 (2004) 848–859. 10.1210/en.2003-1014 [PubMed: 14605006]
52. Tella SH, Gallagher JC, Prevention and treatment of postmenopausal osteoporosis, J. Steroid Biochem. Mol. Biol 142 (2014) 155–170. 10.1016/j.jsbmb.2013.09.008. [PubMed: 24176761]
53. Yu X, Botchwey EA, Levine EM, Pollack SR, Laurencin CT, Bioreactor-based bone tissue engineering: the influence of dynamic flow on osteoblast phenotypic expression and matrix mineralization, Proc. Natl. Acad. Sci 101 (2004) 11203–11208. [PubMed: 15277663]
54. Loi F, Córdova LA, Pajarinen J, Lin T, Yao Z, and Goodman SB, Inflammation, fracture and bone repair. Bone 10.1016/j.bone.2016.02.020
55. de Oliveira S, Rosowski EE, & Huttenlocher A (2016). Neutrophil migration in infection and wound repair: going forward in reverse. Nature Reviews Immunology, 16(6), 378.
56. Brown BN, Ratner BD, Goodman SB, Amar S, & Badylak SF (2012). Macrophage polarization: an opportunity for improved outcomes in biomaterials and regenerative medicine. Biomaterials, 33(15), 3792–3802. [PubMed: 22386919]

Statement of Significance

Designed multimodal porosity of 3D printed TCP scaffold allowed a controlled and sustained release of soy isoflavones, genistein and daidzein in both physiological and acidic pH. Presence of genistein showed 90% reduction in *in vitro* bone cancer cell viability and proliferation. Meanwhile, controlled release of genistein, daidzein, and glycitein from 3DP TCP scaffold demonstrated improved osteoblast cell proliferation, viability, and differentiation in static and dynamic flow-perfusion bioreactor. Furthermore, H&E staining at 24 hours post-surgical specimens from rat distal femur model shows neutrophil recruitment at the surgery site was significantly decreased, suggesting the anti-inflammatory property of soy isoflavones. This work provides deeper understanding on the design of a multifunctional scaffold with enhanced *in vitro* chemopreventive, osteogenic and *in vivo* anti-inflammatory ability.

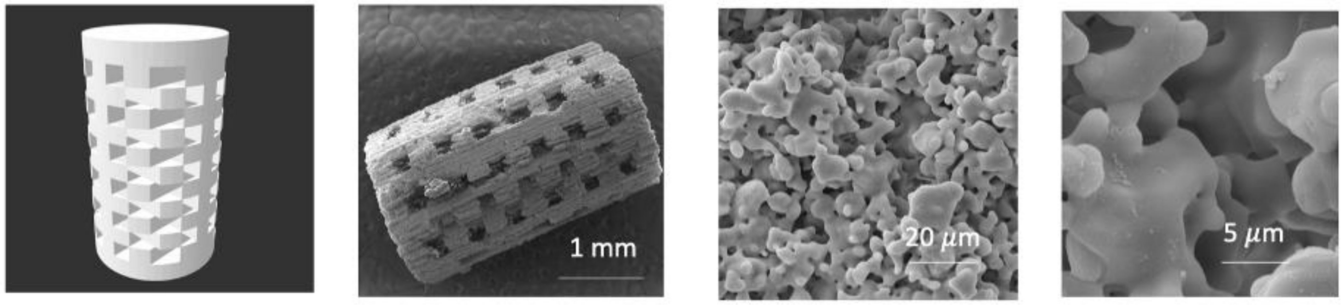

Fig.1.
(left to right) CAD file of the 3DP TCP scaffold with 400 μm designed pores, sintered scaffold, residual micropores of 5–20 μm in sintered scaffold

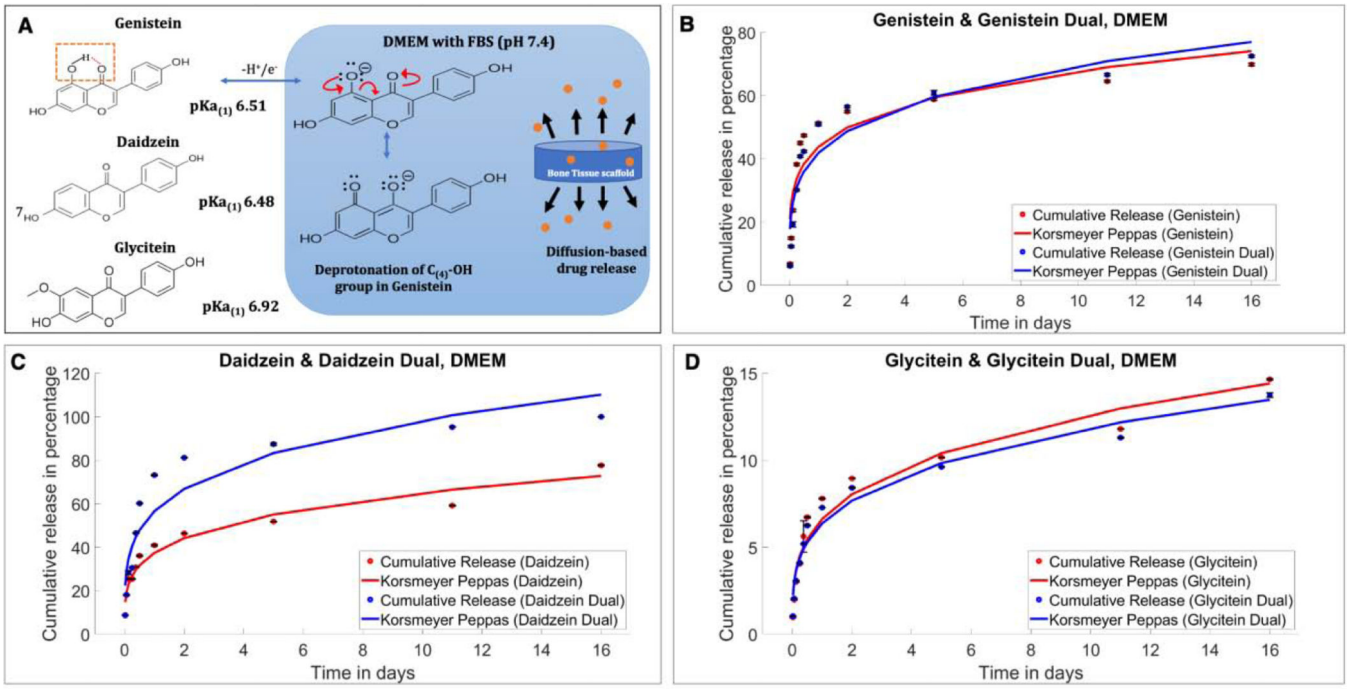

Fig.2.

(A) The acid dissociation constant or pKa values for genistein, daidzein and glycitein are 6.51, 6.48 and 6.92, respectively, indicating that these isoflavones are easily deprotonated at physiological pH of 7.4, resulting in overall higher resonance stability and solubility in physiological pH (B) In vitro cumulative release of genistein in single and combined form fitted in Korsmeyer-Peppas model at DMEM (pH 7.4). A little increment in genistein release has been shown in the presence of other two isoflavones. (C) In vitro cumulative release of daidzein fitted in Korsmeyer-Peppas model showing increased in vitro release in the presence of a second drug in the system. (D) In vitro cumulative release of glycitein fitted in Korsmeyer-Peppas model showing lower cumulative release compared to other two isoflavones.

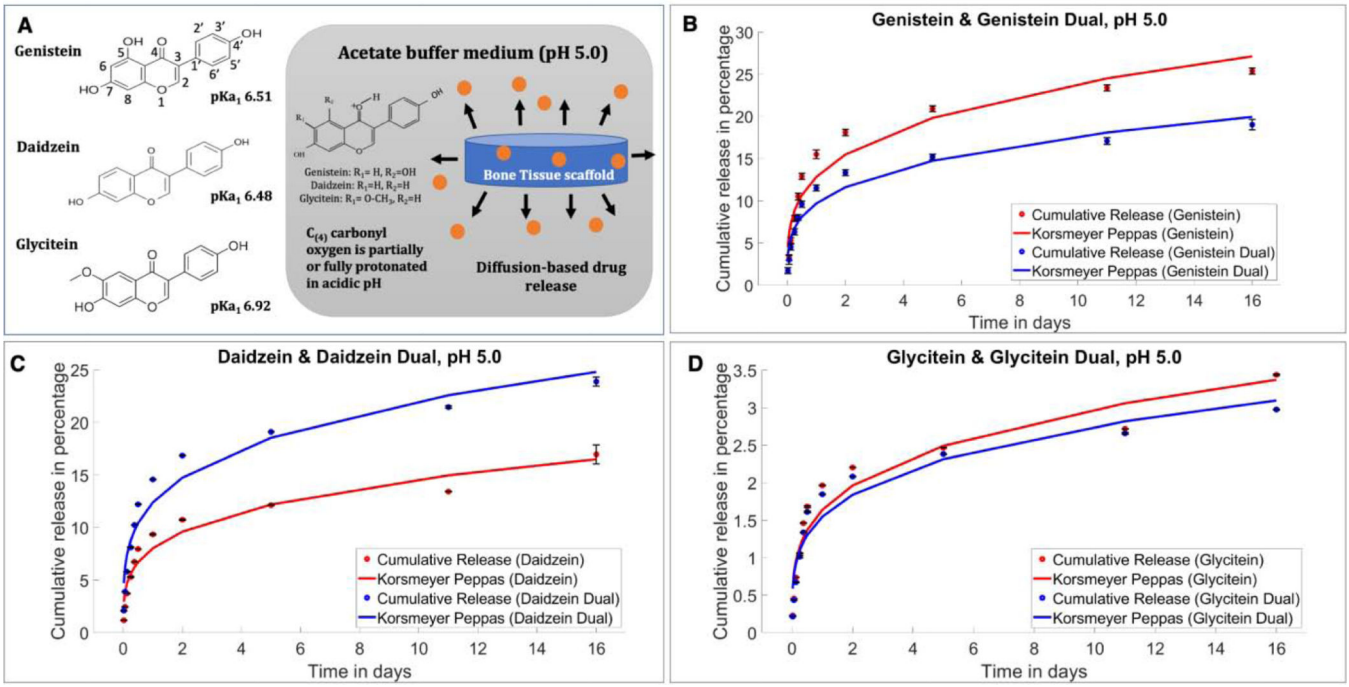

Fig. 3.

(A) At pH 5.0, the isoflavones primarily stay in partially protonated form resulting in lower solubility. (B) In vitro cumulative release of genistein in single and combined form fitted in Korsmeyer-Peppas model at pH 5.0. Increased genistein release can be seen in single drug delivery compared to the combination form. (C) In vitro cumulative release of daidzein fitted in Korsmeyer-Peppas model showing increased in vitro release in the presence of a second drug in the system, unlike the other two isoflavones. (D) In vitro cumulative release of glycitein fitted in Korsmeyer-Peppas model showing lower cumulative release compared to single glycitein delivery.

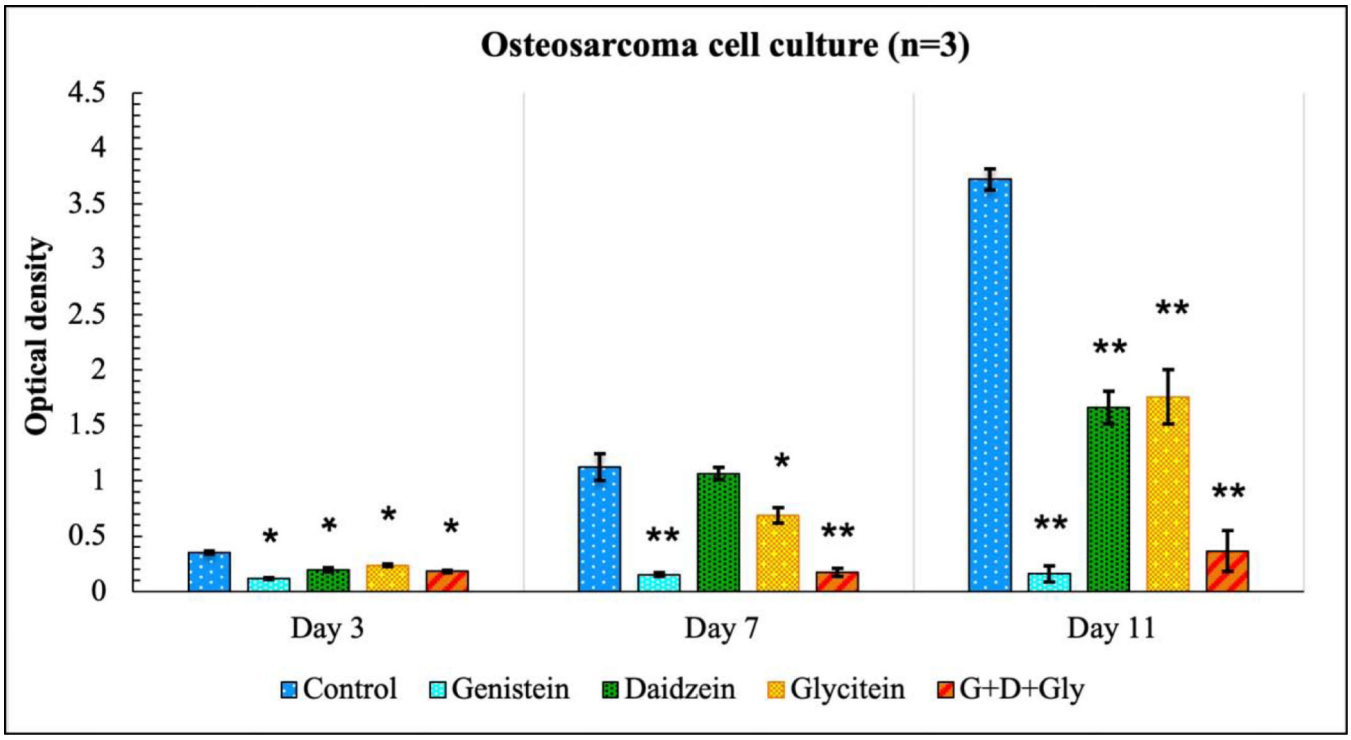

Fig. 4.

MTT assay showing the effects of soy isoflavones loaded 3DP TCP bone tissue engineering scaffolds for in vitro osteosarcoma cell proliferation in a static condition at day 3, 7 and 11. Lowest osteosarcoma or bone cancer cell viability can be seen in the presence of only genistein, while daidzein and glycitein could not exert a significant chemopreventive effect on day 3 or day 7. Combination of all three isoflavones still showed significant cellular toxicity. [* denotes p-value <0.05, ** denotes p-value <0.0001, statistically significant difference between control and test sample]. [Control: 3D TCP: 3D printed porous TCP scaffold]

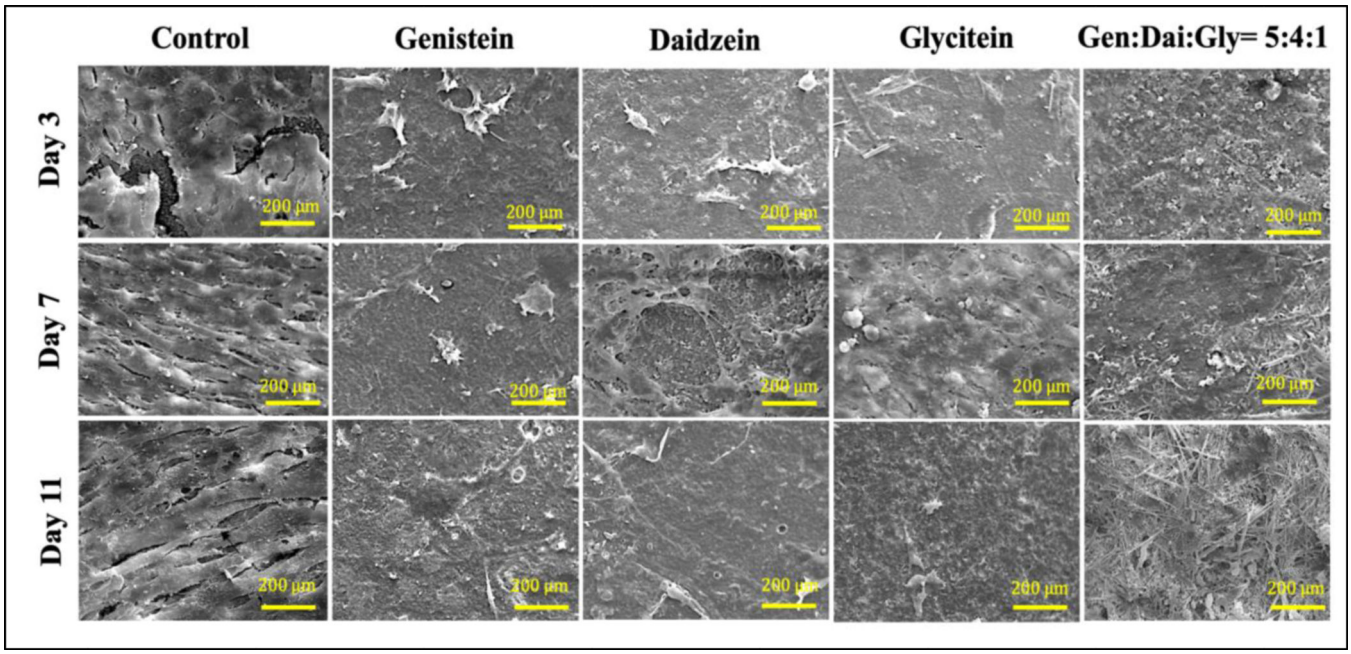

Fig. 5.

FESEM images showing the effects of soy isoflavones loaded 3DP TCP bone tissue engineering scaffolds for in vitro MG-63 cell proliferation in a static condition at day 3, 7 and 11. Layers of bone cancer cells can be seen on TCP scaffold alone, where the presence of genistein exhibits very low cell proliferation suggesting its chemopreventive ability. Although daidzein and glycitein did not have a pronounced effect on MG-63 cells on day 7, the combined effect of three isoflavones showed significant chemopreventive effects in all the time points.

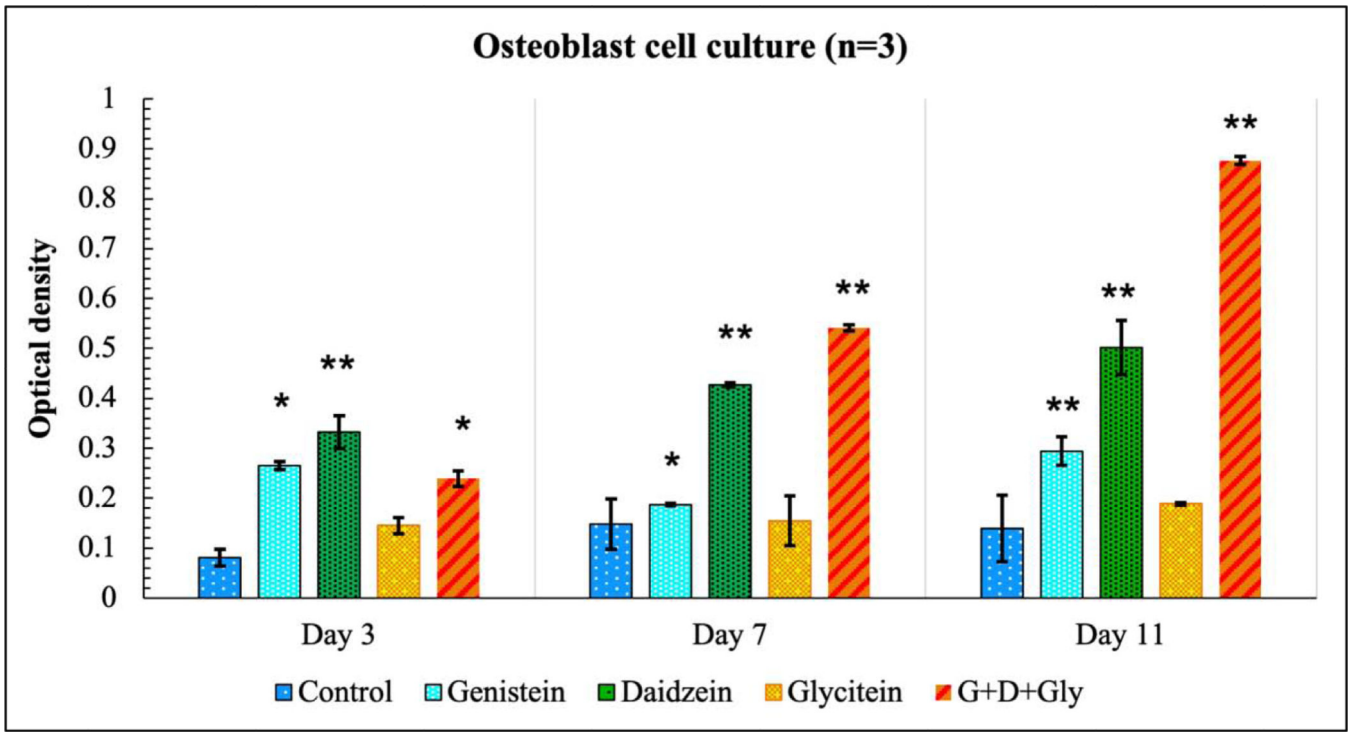

Fig. 6.

MTT assay showing the effects of soy isoflavones loaded 3DP TCP bone tissue engineering scaffolds for in vitro osteoblast cell proliferation in a static condition at day 3, 7 and 11. Daidzein, being osteogenic increased the hFOB cell viability in day 3, 7 and 11. The combined release of all three isoflavones showed the highest cell viability among all compositions. [* denotes p-value <0.05, ** denotes p-value <0.001, significant difference between control and test sample]. [Control: 3D TCP: 3D printed porous TCP scaffold]

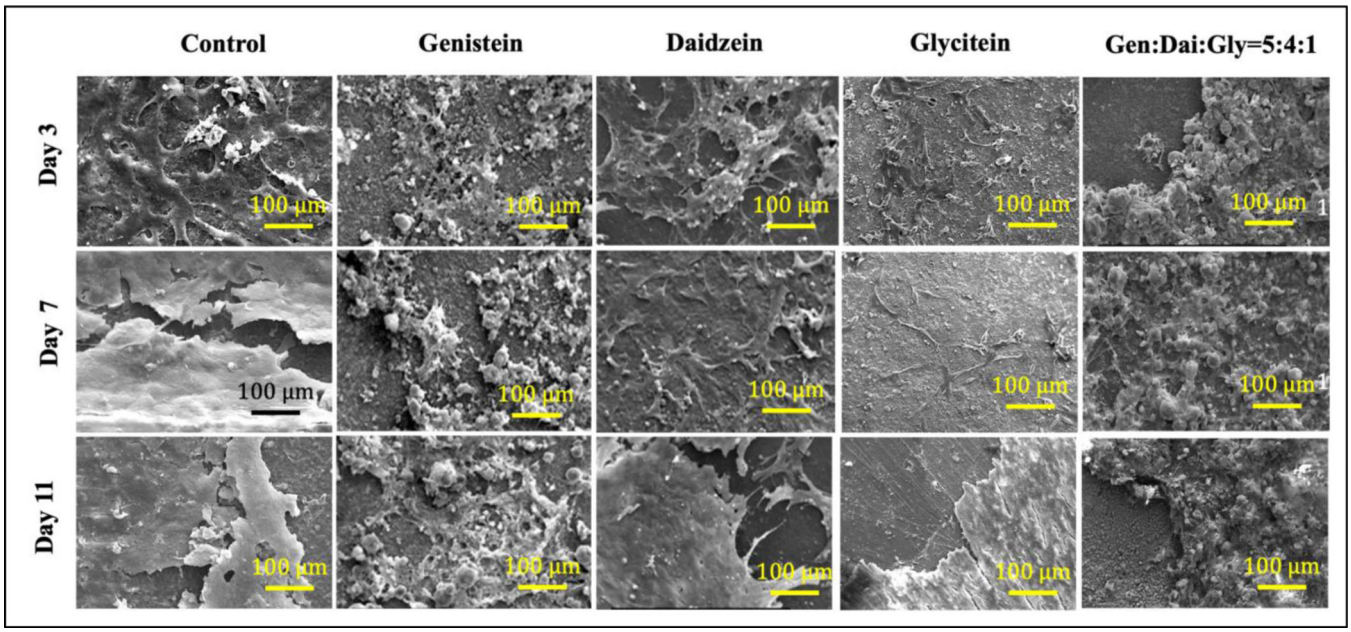

Fig. 7.

FESEM images showing the effects of soy isoflavones loaded CaP bone tissue engineering scaffolds for in vitro osteoblast cell proliferation at day 3, 7 and 11.

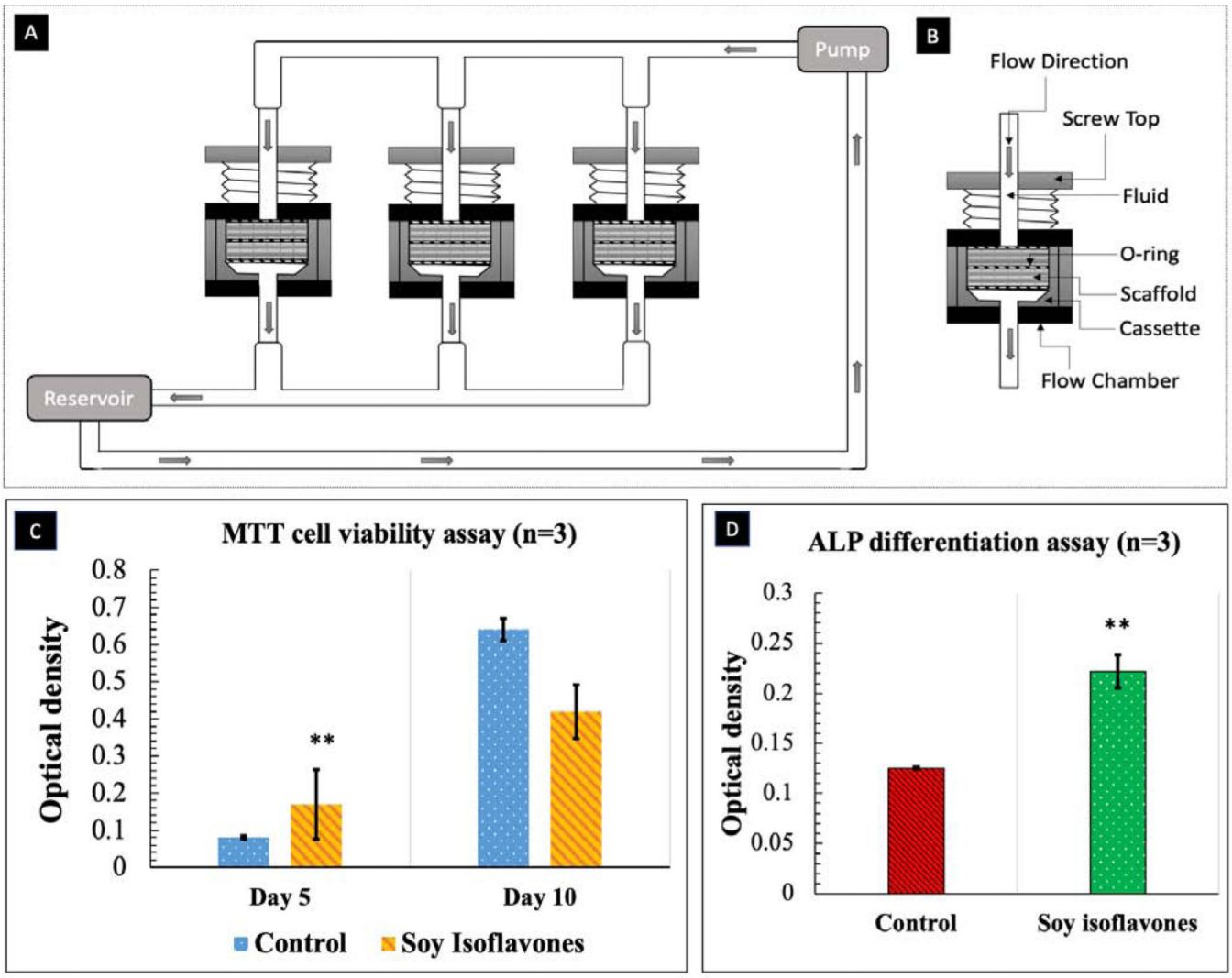

Fig. 8.

(A) Schematic diagram of perfusion flow bioreactor (B) Flow chamber and cassette diagram. Illustrated here is the design of the flow chamber in the flow perfusion culture system. The scaffold is press-fit into a custom-machined polycarbonate cassette. These cassettes are machined specifically to the diameter of the scaffolds used and can be made with different diameters for investigating scaffolds of varying dimensions. The cassette with scaffold is sealed in place by two neoprene O-rings above and below the cassette. This three-part assembly (cassette and two O-rings) is then held in place by a polycarbonate screwtop. Silicone tubing then connects each of these flow chambers to the pump and reservoir systems. (C) MTT assay (n=3) showing the effects of soy isoflavones loaded 3DP TCP bone tissue engineering scaffolds for in vitro osteoblast cell proliferation in a flow perfusion bioreactor at day 5 and 10.)[** denotes p-value <0.0001, statistically significant difference between control and test sample]. [Control: 3D TCP: 3D printed porous TCP scaffold] (D) ALP assay (n=3) showing the effects of soy isoflavones loaded 3DP TCP bone tissue engineering scaffolds for in vitro osteoblast cell differentiation in a flow perfusion bioreactor

at day 10.[** denotes p-value <0.0001, statistically significant difference between control and test sample]. [Control: 3D TCP: 3D printed porous TCP scaffold]

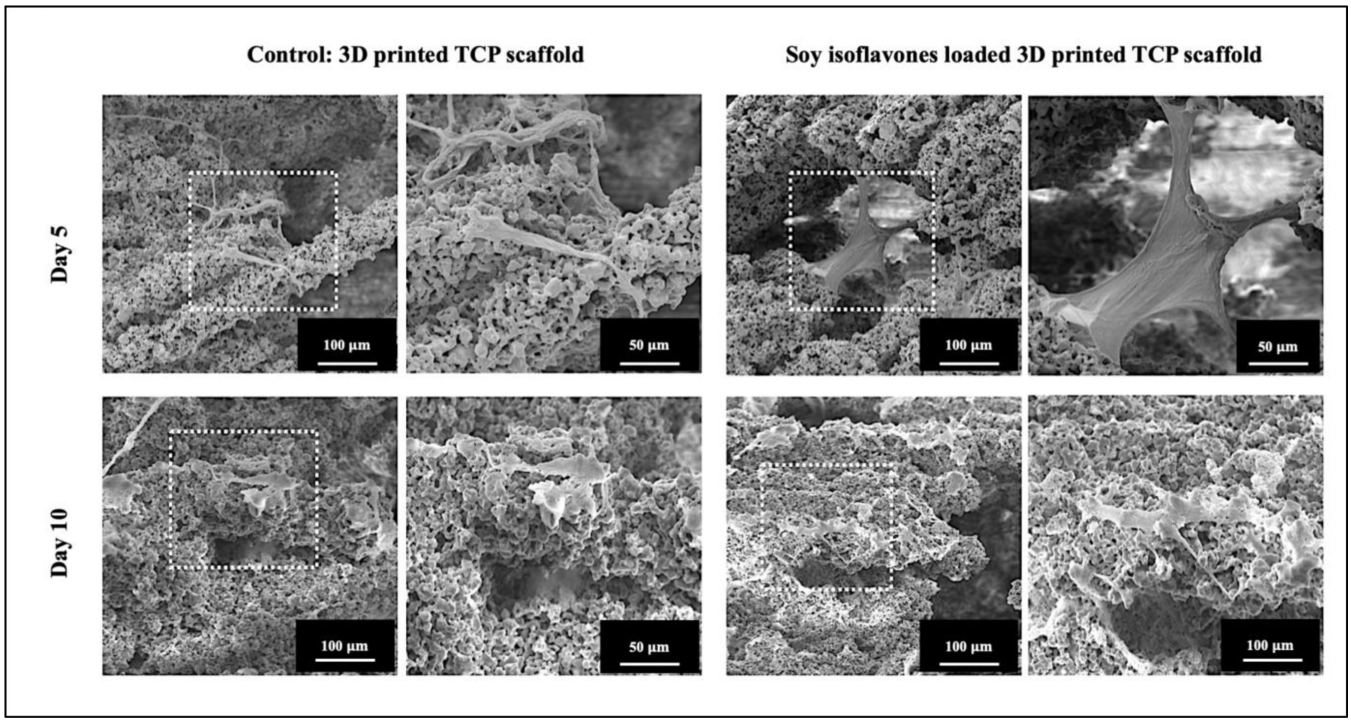

Fig. 9.

FESEM images showing the effects of soy isoflavones loaded 3DP TCP bone tissue engineering scaffolds for in vitro osteoblast cell proliferation in a flow perfusion bioreactor at day 5 and 10.

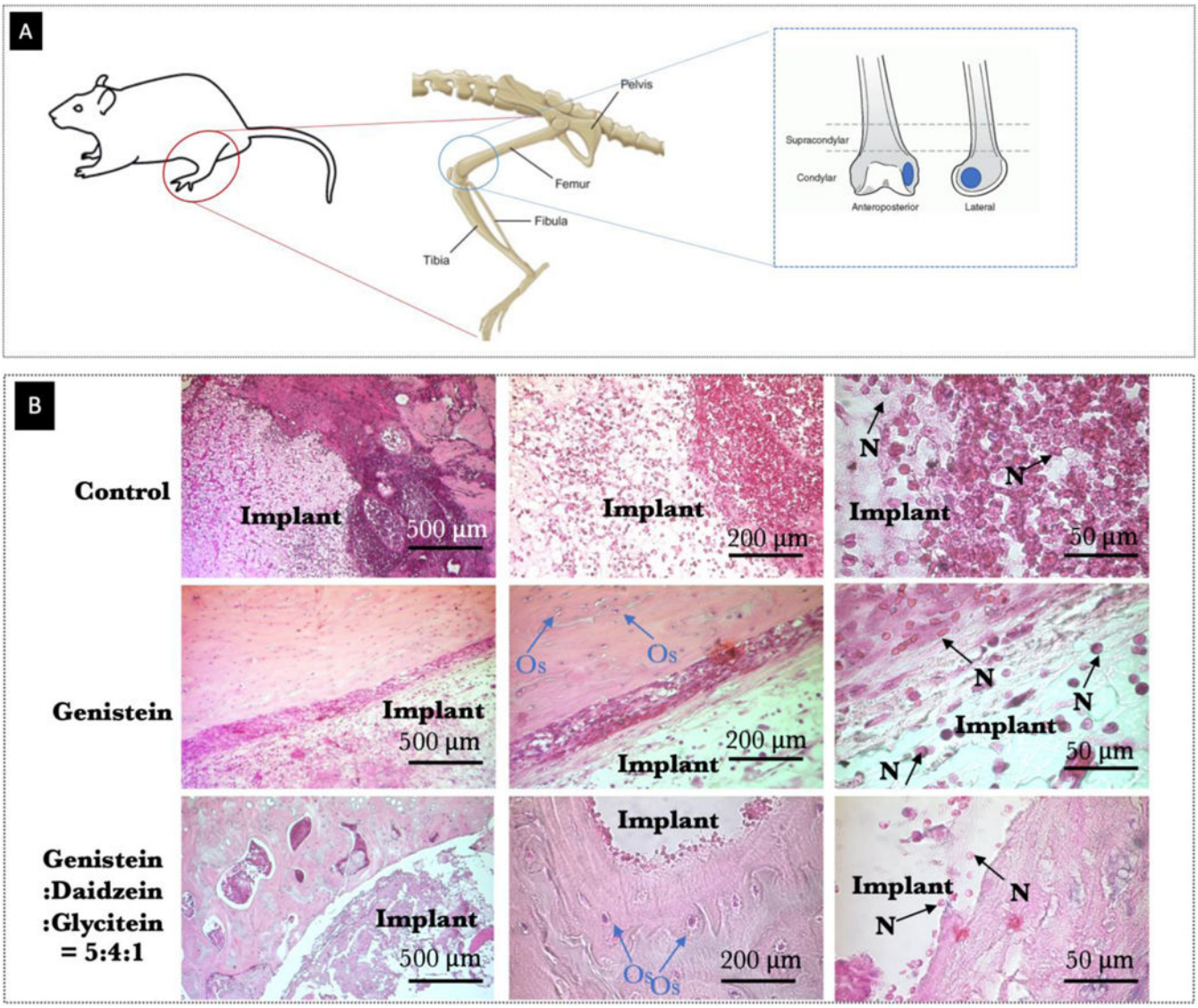

Fig. 10.

(A) Schematic representation of the surgical procedure and the 3D printed TCP scaffold (diameter of 3 mm and height of 5 mm) utilized for implantation (B) Optical microscopy images of decalcified tissue-implant specimens after H&E staining showing inflammatory cell recruitment after 24 days of surgery in rat distal femur model. Blue and black arrow show neutrophil recruitment and presence of osteocytes, respectively.

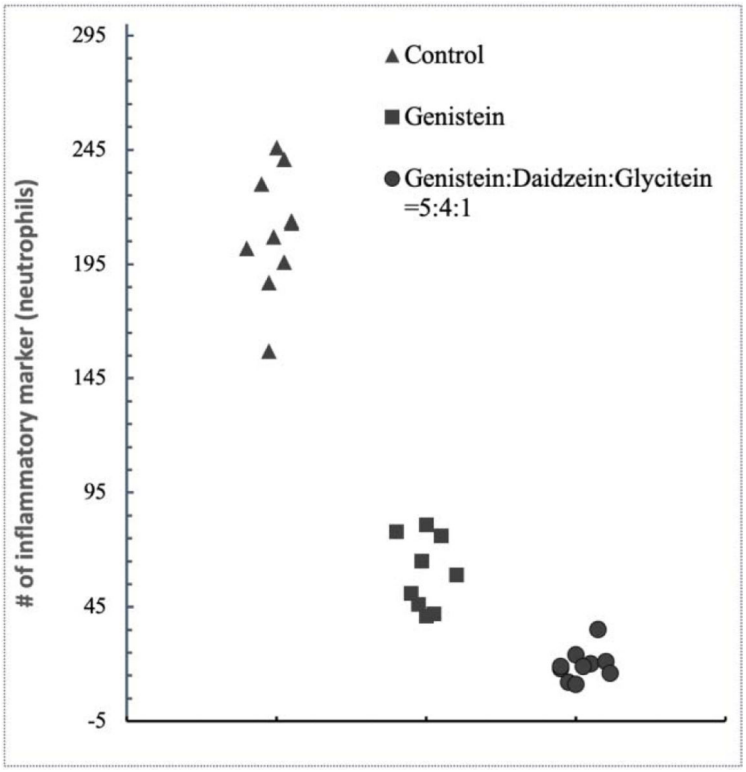

Fig. 11.

Scatter plot obtained by imagePro software demonstrating the relative number of neutrophil cells for *in vivo* tissue sections from control, genistein and genistein:daidzein:glycitein=5:4:1 samples (n=10 slides). The imagePro software defined the difference as statistically significant ($p<0.001$).

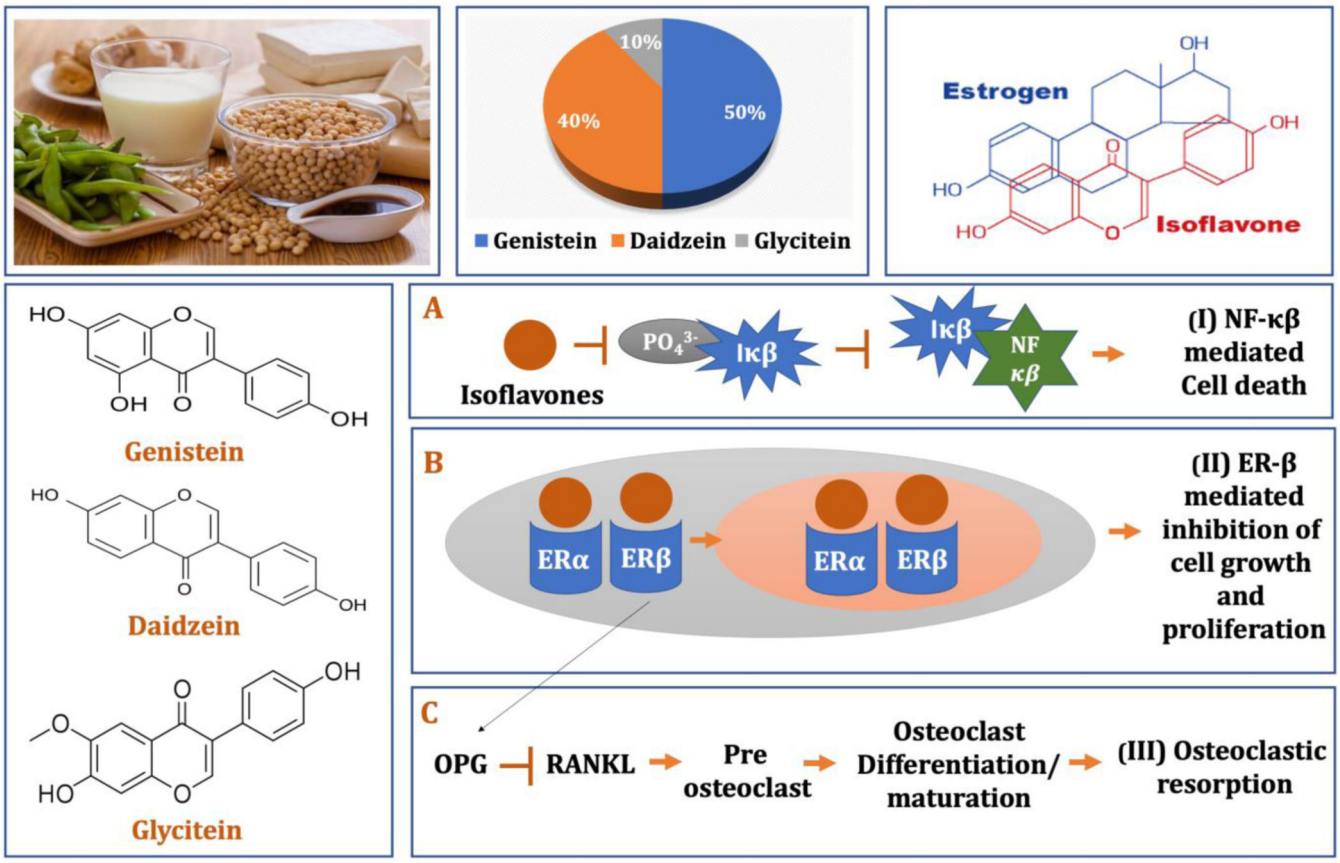

Fig. 12.

The graphical representation shows the dietary sources of soy isoflavones, percentage constituents of isoflavones found in soy foods and similarity of isoflavones to mammalian estrogen. The chemical structure of primary three isoflavones, genistein, daidzein and glycitein are also presented. (A) The possible mechanism of action of soy isoflavones towards chemoprevention and anti-inflammatory activity is demonstrated through NFκβ inhibition pathway [48–49]. (B) Estrogen-mimicking activity of soy isoflavones result in its ability to bind to the estrogen receptor and subsequent ER-β-mediated inhibition of cell growth and proliferation [50]. (C) Isoflavones also suppress osteoclastogenesis through the upregulation of OPG expression, which in turn inhibits RANK-RANKL interactions [51–52].

Table 1:

Effect of soy isoflavone released from 3D printed TCP scaffolds on osteosarcoma cell viability at day 3, 7 and 11 (<70% implies the drug has cytotoxic potential, $p < 0.05$)

	Genistein	Daidzein	Glycitein	Gen:Dai:Gly= 5:4:1
Day 3	33.4 ± 0.39%	55.1 ± 1.3%	66.8 ± 0.7%	51.4 ± 2.1%
Day 7	13.5 ± 0.5%	94.6 ± 0.3%	61.3 ± 0.8%	15.5 ± 0.1%
Day 11	4.3 ±0.4 %	44.6 ± 1.6%	47.2 ± 1.9%	9.8 ± 0.9%

Table 2:

Effect of soy isoflavones released from 3D printed TCP scaffolds on neutrophil recruitment surrounding the implant area after 24 hours of surgery in rat distal femur model (Scoring was done as follows: absent (−), mild (+), moderate (++), and severe (+++), n= 10 slides). The imagePro software defined the inflammatory and osteogenic marker difference to be significant at $p<0.001$.

Composition	Neutrophils recruitment
Control (3DP TCP)	+++
Treatment 1: Genistein loaded 3DP TCP	++
Treatment 2: Soy isoflavone (Genistein:Daidzein:Glycitein = 5:4:1) loaded 3DP TCP	+